



# HHS Public Access

Author manuscript

*Adv Drug Deliv Rev.* Author manuscript; available in PMC 2014 December 01.

Published in final edited form as:

*Adv Drug Deliv Rev.* 2013 December ; 65(15): 1921–1932. doi:10.1016/j.addr.2013.07.007.

## Peroxidase-mediated Biodegradation of Carbon Nanotubes *in vitro* and *in vivo*

Gregg P. Kotchey<sup>a</sup>, Yong Zhao<sup>a</sup>, Valerian E. Kagan<sup>a,b</sup>, and Alexander Star<sup>\*,a</sup>

<sup>a</sup>Department of Chemistry, University of Pittsburgh, Pittsburgh, Pennsylvania, USA

<sup>b</sup>Department of Environmental and Occupational Health, University of Pittsburgh, Pittsburgh, Pennsylvania, USA

### Abstract

As a result of their unique electronic, optical, and mechanical properties, carbon nanotubes (CNTs) have been implemented in therapeutic and imaging applications. In an idealized situation, CNTs would be disposed of after they transport their theranostic payloads. Biodegradation represents an attractive pathway for the eliminating of CNT carriers post-delivery and may be integral in catalyzing the release of the cargo from the delivery vehicle. Accordingly, recent research efforts have focused on peroxidase-driven biodegradation of CNTs. In this review, we not only summarize recent efforts to biodegrade CNTs in the test tube, *in vitro*, and *in vivo*, but also attempt to explore the fundamental parameters underlying degradation. Encouraged by the *in vivo* results obtained to date, we envision a future, where carbon-based nano-containers, which are specifically designed to target organs/cells, deliver their cargo, and biodegrade *via* peroxidase-driven mechanism, will represent an attractive therapeutic delivery option in nanomedicine.

### Keywords

Biodegradation; carbon nanotubes; graphene; nanoparticles; peroxidases; drug delivery

## 1. Introduction

Structurally, single-walled carbon nanotubes (SWCNT) can be envisioned as a single sheet of graphene rolled seamlessly into a cylinder; multiwalled carbon nanotubes (MWCNTs) are comprised of concentrically nested SWCNTs of increasing diameter. Because their geometries are characterized by nanometer-sized diameters (*i.e.* from 0.4 to 3 nm and 2 to 100 nm for SWCNTs and MWCNTs, respectively) and a length of several micrometers [1], carbon nanotubes (CNTs) possess a high aspect ratio. Moreover, CNTs are endowed with unique electronic [2], optical [3], and mechanical properties [4], which enable this sp<sup>2</sup>-

© 2013 Elsevier B.V. All rights reserved

\*Email of Corresponding Author: astar@pitt.edu.

**Publisher's Disclaimer:** This is a PDF file of an unedited manuscript that has been accepted for publication. As a service to our customers we are providing this early version of the manuscript. The manuscript will undergo copyediting, typesetting, and review of the resulting proof before it is published in its final citable form. Please note that during the production process errors may be discovered which could affect the content, and all legal disclaimers that apply to the journal pertain.

hybridized allotrope of carbon to be employed for diverse applications such as electronics [5], sensors [6, 7], composite materials [8], energy conversion devices [9], and medicine [10, 11]. This review article is related to their drug delivery application and will examine issues related to *in vitro* and *in vivo* biodegradation of CNTs catalyzed by peroxidases.

### 1.1. CNTs and Drug Delivery

A vast variety of nanoparticles (NPs) composed of metals, metal oxides, quantum dots (QDs), polymers, and carbon (*e.g.* carbon nanotubes and graphene) are receiving increasing interest over the recent years due to their potential *in vivo* therapeutic or imaging applications [12–14]. As a result of their high surface area and unique optical and electronic properties, CNTs have the potential of becoming a highly efficient delivery vehicle for drugs and biomolecules [14]. Because as-prepared CNTs are hydrophobic, to enhance their dispersibility in aqueous environments and thereby implement this carbon-based nanomaterial for biomedical applications [15], CNTs must be modified by either covalent or noncovalent means; this action will not only enhance biodispersibility but also biocompatibility of CNTs. Once rendered biodispersible and biocompatible, the high surface area of the CNTs presents an attractive platform for therapeutic delivery, where peptides, nucleic acids, proteins, and drugs could be (1) stored in the large inner-tubular volume; (2)  $\pi$ - $\pi$  stacked to the walls; and/or (3) covalently conjugated to defect sites on the walls/edges of this carbon-based nanomaterial [16]. Moreover, CNTs are proficient at entering the nuclei of cells [17], which may render this nanomaterial integral for gene therapy applications. Interestingly, the near-infrared (NIR) biological transparency window, which occurs in the range of 800 to 1400 nm, falls within the region where SWCNTs strongly absorb and emit light (*i.e.* 800 to 1600 nm) [14]. As a result, SWCNTs have been employed for photothermal therapy, photoacoustic imaging, and Raman detection/imaging [14].

The primary hindrance to employing CNTs for biomedical applications entails potential toxicity issues that include oxidative stress and inflammatory pathways [18]. By controlling physicochemical properties such as length and degree of functionalization and pharmacological parameters such as dosing, the toxicological properties of CNTs can be mitigated [19]. Moreover, *in vitro* and *in vivo* studies have been implemented to acquire insight into the biological transformation and long-run fate of CNTs; these studies have demonstrated that there exist pathways to mitigate toxicity through the biodegradation of CNTs. These findings are applicable to CNT drug delivery vehicle, where biodegradation may either catalyze the release of the cargo conjugated to the CNT carrier or destroy the CNT delivery vehicle post-release thereby mitigating potential toxicity. Accordingly, this article will guide the reader through these recent *in vitro* and *in vivo* efforts to biodegrade CNTs.

## 2. *In vitro* Degradation of CNTs Outside Living Systems

Recent reports have demonstrated that the plant peroxidase, horseradish peroxidase (HRP) [20–25], and the animal peroxidases, myeloperoxidase (MPO) [25–28] and eosinophil peroxidase (EPO) [29], catalyze the degradation/biodegradation of carbon nanomaterials. In this section, we investigate in test tube examples of and provide plausible explanations of enzyme-catalyzed degradation of CNTs. This section will function as a tutorial for later

sections in which cellular and *in vivo* studies that demonstrated biodegradation of CNTs are explored.

### 2.1. HRP – The Model Peroxidase System for CNT Degradation

In an early study, we demonstrated that HRP catalyzed the degradation of carboxylated SWCNTs in the presence of H<sub>2</sub>O<sub>2</sub> [20]. HRP, which has been employed in applications ranging from biotechnology to bioremediation [30], represents a classical secretory plant peroxidase that is derived from the horseradish plant (*A Armoracia rusticana*) [31]. This monomeric enzyme consists of a noncovalently bound ferriprotoporphyrin IX prosthetic heme group [31] as its active site. When HRP is in its native, resting state, this group is in the ferric, Fe(III), form. The heme center is converted into an oxo-ferryl iron (Fe<sup>4+</sup>=O) and a porphyrin  $\pi$  cation radical referred to as Compound I *via* a protein-assisted mechanism upon reaction with hydrogen peroxide (H<sub>2</sub>O<sub>2</sub>), which is reduced back to the ferric resting state by the peroxidase cycle (Figure 1A) [30].

In a following mechanistic investigations, we demonstrated that only SWCNTs that contain oxygen moieties/defect sites underwent degradation; pristine SWCNTs were not observed to degrade over the same time period [21]. The introduction of defect site that consist of oxygen functionalities (*e.g.* carboxyl, carbonyl, and hydroxyl groups) by strong oxidizing agents, represents one common methodology employed to enhance the biocompatibility of CNTs [32, 33]. Carboxyl groups are attached to the graphitic backbone by one bond [34]; therefore, because it is necessary to cleave only a single bond, CNTs functionalized with these groups would therefore appeared most susceptible to enzymatic oxidation *versus* other functional groups. Moreover, the ability of HRP to preferentially react on carboxylated CNTs was supported by the different degradation behavior of carboxylated MWCNTs [22, 23]. As the carboxylation process can only impart functional groups to the outer layers of MWCNTs, the more pristine inner layers failed to be completely degraded after the exfoliation of outer layers.

As previously mentioned, pristine CNTs were not observed to degrade over the period of analysis [25]. This may be attributed to two reasons. The first explanation is related to the overall dispersity of CNTs in an aqueous media; because pristine CNTs are intrinsically hydrophobic, there exists a strong tendency for nanotubes to aggregate into bundles, ropes, and networks as a result of van der Waals forces. To counteract these effects, CNTs have been modified by numerous covalent and noncovalent modifications to render this nanomaterial more dispersible in an aqueous environment [15]. To this end, CNTs have been functionalized employing several methodologies, including: (1) the creation of defect-sites *via* strong oxidant chemistry, (2) covalent chemistry performed on sidewall, (3) attachment of pyrene derivatives *via*  $\pi$ - $\pi$  interactions, and (4) noncovalent wrapping utilizing surfactants/amphiphiles, polymers, and biopolymers [35]. These techniques often yield a high-quality dispersion, which is composed mainly of individualized nanotubes with the remainder consisting of small bundles; Coleman and coworkers demonstrated that the quality of these dispersions scale with the  $\zeta$ -potential of the dispersion [36]. As the  $\zeta$ -potential increases, the electrostatic repulsion of the functional groups imparted by the dispersing agent/*via* covalent modification is sufficient to overcome the attractive van der

Waals interactions of the CNTs [37]. While the direct role of bundling on degradation has not yet been examined, all studies that reported degradation were conducted on functionalized CNTs that demonstrate minimal bundling.

The second factor, which is also related to dispersibility, entails nanotube-enzyme interactions. When dispersed in an aqueous media, the negative charge of carboxyl groups on the covalently functionalized SWCNTs may facilitate degradation by encouraging the proper orientation/proximity of the peroxidase enzyme's heme active site to the SWCNT substrate, which has been demonstrated by molecular modeling studies. Due to electrostatic interactions, the negatively charged carboxylated CNTs would orient themselves toward a positively charged arginine residue, Arg178, which is positioned near HRP's heme site (Figure 1B) [21]. On the other hand, pristine SWCNTs were predicted to orient themselves towards the distal end of the enzyme away from the active heme site thereby failing to undergo degradation [21].

Even if the functionalized CNTs are well dispersed and properly oriented relative to the enzyme's active site, oxidation/degradation is not expected to proceed unless the standard potential of the reactive intermediates of HRP exceed the value for CNTs. For example, the reactive intermediates of HRP have a mean standard potential ( $E^0$ ) of +0.884 V (Table 1) [38] while SWCNTs have a work function ( $V$ ) under vacuum of ~5 eV and a corresponding standard potential ( $E^0$ ) of +0.5 V [39, 40]. Therefore, the reactive intermediates of HRP possess more positive redox potentials and are stronger oxidants than SWCNTs [25]. Consequently, SWCNTs should theoretically be spontaneously oxidized through the donation of electrons from their valence band to these mediators.

HRP represents a promising model system for fundamental studies and may be relevant for environmental applications relating to carbon nanotube bioremediation. For applications relating to nanotoxicity and drug delivery, more physiologically relevant peroxidases were examined.

## 2.2. MPO and EPO – Peroxidases that Generate Hypohalous Acids

In collaboration with others, we have further expanded the *in vitro* degradation of CNTs to a series of peroxidases derived from animals including humans. A representative study demonstrated that human myeloperoxidase (hMPO) degraded carboxylated SWCNTs [26]. MPO consists of a homodimeric protein that is predominately expressed in granules of neutrophils (*i.e.* a type of leukocytes). In response to the phagocytosis of bacterium, MPO is released from these granules primarily into phagolysosomal compartment during which this peroxidase enzyme functions as a bactericide through the generation of both reactive intermediates (*i.e.* formed *via* the peroxidase cycle) and oxidants that are formed during the halogenation cycle (Figure 1A) [31, 41–43]. During the halogenation cycle, MPO demonstrates the ability to oxidize  $\text{Cl}^-$ ,  $\text{Br}^-$ , and the pseudohalide,  $\text{SCN}^-$  at high rates; during the process, these substrates donate two electrons to Compound I to generate the ferric form of the enzyme and, in turn, are converted to the corresponding (pseudo)hypohalous acids (HXO, such that  $\text{X} = \text{Cl}, \text{Br}, \text{SCN}$ ) [44].

After incubating carboxylated SWCNTs with hMPO in the presence of both H<sub>2</sub>O<sub>2</sub> and Cl<sup>-</sup> for 24 h, the dispersion appeared almost clear in color (Figure 2A). Moreover, the SWCNTs underwent structural deformation including both a decrease in size as revealed by dynamic light scattering (DLS) (Figure 2B) and an increase in defects as evidenced by the increase in the D/G band ratio, which was determined by Raman spectroscopy (Figure 2C). Degradation of the SWCNTs was also confirmed by the suppression of the metallic (M<sub>1</sub>) and semiconducting (S<sub>2</sub>) transition bands that characterize the vis-NIR absorption spectra for SWCNTs (Figure 2D). The control experiment, which excluded Cl<sup>-</sup> and therefore relied only on the reactive intermediates formed during the peroxidase cycle, demonstrated markedly less SWCNT degradation thereby suggesting the important role of the strong oxidant, hypochlorous acid (HClO), in the degradation process; the *in vitro* study by Vlasova *et al.* confirmed this finding [27]. Presumably, the synergetic effects of hypochlorite and the reactive intermediates of MPO facilitated a much higher efficiency of CNT degradation for the MPO/H<sub>2</sub>O<sub>2</sub>/Cl<sup>-</sup> system *versus* the HRP/H<sub>2</sub>O<sub>2</sub> system. Of importance, small oxidants like HClO has the ability to diffuse from active site and oxidize CNTs; the more bulky reactive intermediates, on the other hand, must be in close enough proximity of the CNT to promote degradation. Moreover, the enzyme-catalyzed oxidation of CNTs may be in competition with other substances that have lower redox potential (*i.e.* more reductive), as shown in our recent study, where the enzymatic degradation of SWCNTs was mitigated by antioxidants added to the system [45].

For MPO, amino acid residues, Glu242, Asp94 and Met243, are covalently bound to the ferriprotoporphyrin IX heme group [31], and molecular simulations suggested the existence of two potential interaction sites for CNT binding depending on their functionality [26]. For acid treated SWCNTs, the positively charged arginine residues (*i.e.* Arg 294, 307, and 507), which reside near the proximal end of the heme group, strongly interacted with the negatively charged carboxylated nanotubes; this area also contained the catalytically active tyrosine residues, Tyr293 and 313 (Figure 1C) [26]. Alternatively, pristine SWCNTs appeared to favor a second binding site, which exists at the distal end of the heme group away from the tyrosine residues [26].

EPO also facilitated the degradation of CNTs. EPO, which is expressed by eosinophils (*i.e.* a type of leukocytes), assists in the destruction of invading parasites. Because, in general, parasites are larger than bacteria, eosinophils attach to these species and exocytose their granule contents, which is composed of EPO at 40% by mass. Interestingly, EPO possesses a 70% amino acid homology with MPO but weighs roughly half of latter enzyme (*i.e.* 69.8 kDa versus 144 kDa, respectively) [44], and inflammation of the human lung is characterized by the presence of EPO [29]. Like MPO, EPO contains a modified heme groups that are composed of ferriprotoporphyrin IX as its active site and therefore can generate reactive intermediates by the peroxidase cycle and hypohalous acids by the halogenation cycle [44]. It is important to note that because of the differences in the active-site topology and binding sites between MPO and EPO, the redox potentials of the enzymes (Table 1) does not always correlate with the rate constants that the enzymes exhibit for a given (pseudo)halide [44]. For example, at neutral pH and given physiological concentrations of Cl<sup>-</sup>, Br<sup>-</sup>, and, SCN<sup>-</sup>, MPO primarily generates HClO and HSCNO

although it has the ability to oxidize  $\text{Br}^-$ .  $\text{HBrO}$  and  $\text{HOCl}$  and primarily produced by EPO despite this enzyme being a strong enough oxidant to convert  $\text{Cl}^-$  to  $\text{HClO}$ , [44]. The reduction potentials for these (pseudo)hypohalous acids at pH 7 are denoted by Table 2 [44].

For the *in vitro* experiment, carboxylated SWCNTs were incubated with human EPO (hEPO) under physiological condition with constant addition of  $\text{H}_2\text{O}_2$  and  $\text{NaBr}$ . During the 96 h incubation, degradation of the SWCNTs was visually observed by a gradual color fading of the SWCNT suspension. A decrease in both the  $\text{S}_2$  characteristic band for SWCNTs in the NIR spectra and the Raman-derived D/G band ratio was observed, which suggested the degradation of SWCNTs under EPO oxidation, which was also confirmed by transmission electron microscopy (TEM). Therefore, the reactive intermediates and  $\text{HBrO}$  acid generated by EPO through the peroxidase and halogenation cycles, respectively, successfully resulted in the degradation of oxidized nanotubes. Significantly, when lactoperoxidase (LPO) was incubated with  $\text{H}_2\text{O}_2$  and  $\text{Br}^-$ , CNT degradation was observed confirming the strong oxidizing role of  $\text{HBrO}$  [27].

For EPO, two binding sites were identified both of which are stabilized by the electrostatic interactions between the positively charged arginine residues (*i.e.* Arg205, Arg207 and Arg209 for binding site 1 and Arg94 and Arg99 for binding site 2) and the negatively charged oxygen-containing functionalities on oxidized SWCNTs (Figure 1D) [29]. Of these two sites, binding site 1 was identified to be located on the same side as the catalytic site, appeared to be closer to the entrance of the catalytic site *versus* binding site 2, and overlapped with one of the bromide ion binding sites. Consequently, these cumulative results indicate that binding site 1 of EPO was the preferred location for biodegradation of oxidized SWCNTs [29].

### 3. *In vitro* Degradation of CNTs in Cells

#### 3.1. Factors that Facilitate *in vitro* Degradation in Cellular Culture

Having had success with enzyme-catalyzed degradation of CNTs in the test tube, cellular studies were performed to elucidate the effect of innate degradative enzymes of the cell on CNTs. To this end, the *in vitro* degradation of CNTs in cell culture has been thus far investigated [26, 29]. The results demonstrated that significant degradation of CNTs was typically observed in granulocytes such as neutrophils and eosinophils, and the degradation was associated with active oxidases and peroxidases that are rich in the aforementioned cells together with reactive intermediates, which are considered to be key factors for CNT degradation by cells.

**3.1.1. Oxidative Stress Induced by CNTs**—It is commonly accepted that the cytotoxicity of nanoparticles such as CNTs is largely derived from oxidative stress resulting from their small size and large specific surface area [46–48]. Moreover, the oxidative stress also arises from increased levels of reactive oxygen species (ROS) that include superoxide radical anions and hydroxyl radicals. As a natural byproduct of cellular respiration process in mitochondria, the ROS are normally balanced by a series of anti-oxidant enzymes. However, the cellular homeostasis can be disrupted when the intracellular ROS levels are significantly levitated by environmental stress (*e.g.* exposure to nanoparticles), thereby

leading to oxidative stress. It is believed that nanoparticles can trigger the formation of ROS through two different pathways [49]. Some transition metal-based nanoparticles can catalyze decomposition of peroxides and form ROS directly such as the Fenton reaction triggered by iron catalytic nanoparticles from unpurified SWCNTs [50]; while in more general cases, the ROS are generated by phagocytic cells of the immune system (*i.e.* neutrophils, eosinophils, and macrophages) in response to the extrinsic nanoparticles. When phagocytes actively internalize nanoparticles, the massive ROS generation process is considered to be NADPH oxidase-dependent [49, 51], where upon activation, NADPH oxidase ensembles at the phagolysosomal membrane and transfers electrons to oxygen to form superoxide in a process known as “oxidative burst” [52]. In turn, superoxide anions will dismutate to  $H_2O_2$  [53], which is an initiator of the aforementioned peroxidase cycle of MPO in neutrophils and EPO in eosinophils. CNTs, in particular, because of their large surface activity, are highly likely to induce oxidative burst.

**3.1.2. Role of Oxidative Stress to the *in vitro* Degradation of CNTs**—It is commonly thought that oxidative stress triggers cell damage and death, and this phenomenon may be the cause of many diseases and cancers [54, 55]. However, the beneficial effects of oxidative stress are receiving more and more attention in recent years as studies revealed the important immune functions of ROS in “oxidative signaling,” which activates the inflammatory response in phagocytic cells, as well as in the attack and degradation of pathogens [49, 56]. The massive generation of strong ROS in response to pathogen engulfment has a large enough oxidative potential to break C-C and C-H bonds in bacteria and viruses thereby leading to their degradation. This oxidative clearance of pathogens also applies to degradation of carbonaceous nanomaterials including CNTs as they share similar sizes and elemental compositions with bacteria or viruses.

The *in vitro* degradation of CNTs is more likely to occur in the activated phagocytic cells with high oxidative stress. As demonstrated by in test tube results, innate peroxidases, such as MPO in neutrophils and EPO in eosinophils, play a pivotal role in oxidative degradation of CNTs. Under natural inflammatory response, neutrophils are attracted and activated by chemoattractants at the inflammatory sites, and MPO is released thus being able to act both intra- and extra-cellularly [57].  $H_2O_2$ , which originated from NADPH oxidase, forms inside the phagosome, activates MPO, and leads to the production of reactive enzymatic intermediates and oxidants (*e.g.* hydroxyl radicals,  $HClO$ , *etc.*) [53], both of which are responsible for CNT degradation. As a result, the phagosomes of the phagocytes provide the exact environment facilitating the degradation of CNTs as simulated under test tube conditions. Both  $H_2O_2$ -generating enzyme (*e.g.* NADPH oxidase) and oxidative peroxidase are essential factors for the degradation of CNTs inside phagocytes under oxidative stress. The presence of halide ions also facilitates the degradation process by forming strong oxidative hypohalous acids. Finally, in the *in vitro* experiment, chemoattractants and degranulation promoting agent must be added to promote degradation. While chemoattractants activate the phagocytic cells, and degranulation promoting agent (*e.g.* cytochalasin B) trigger the release of peroxidase.

**3.1.3. Cellular Internalization of CNTs**—The *in vitro* degradation of CNTs may occur either inside or outside of the cells depending on the distribution of the peroxidase upon cellular activation. If the peroxidase is localized mainly inside of the cells, then CNTs must be pre-opsionized for efficient internalization. Opsonization can be achieved by functionalization of CNTs with immunoglobulins, which specifically target receptors on phagocytes [58]. For example, in our previous study of CNT degradation in neutrophils [26], most of the MPO was translocated into the intracellular phagolysosomal space, where degradation ensued. Therefore, the nanotubes were targeted with IgG for enhanced cellular uptake. A significant increase in uptake and degradation of IgG-nanotubes by neutrophils occurred relative to non-functionalized nanotubes. Additionally, coating with specialized “eat-me” signals such as phosphatidylserine also makes CNTs recognizable by different professional phagocytes [59]. In contrast, in the study of CNT degradation by eosinophils [29], opsonization of CNTs was not required as the biodegradative peroxidase EPO is exocytosed upon cellular activation.

### 3.2. Examples of *in vitro* Degradation

Although a plethora of studies have investigated the cellular uptake of CNTs and their subsequent effects [60–62], only a few studies have addressed the potential cellular clearance of CNTs through biodegradation. Neves, *et al.* reported that the RNA-coated oxidized double-walled CNTs taken up by human prostate adenocarcinoma cells *in vitro* underwent possible defect-induced structural change due to increasing D to G band ratios from the Raman spectra [63]. However, the potential degradation mechanism and the eventual fate of CNTs were not discussed. In order to understand the CNT degradation process in actual living systems, we and others have investigated the *in vitro* degradation in both neutrophils and eosinophils conducted by MPO and EPO, respectively.

**3.2.1. The *in vitro* Degradation of CNTs by Neutrophils**—Human neutrophils, which are rich in MPO, are a type of professional phagocytes that are activated in response of inflammation and engulf pathogens. In an *in vitro* experiment [26], the neutrophils were first treated with fMLP and cytochalasin B to increase the activity of the cells and trigger the release of hMPO. Next, the short, oxidized SWCNTs were functionalized with IgG for their efficient internalization into neutrophils, and they were subsequently incubated with activated neutrophils. The activated neutrophils were shown to undergo an oxidative burst thus generating increased levels of superoxide and H<sub>2</sub>O<sub>2</sub> (Figure 3A, B). Raman microscopy confirmed that IgG-nanotubes were completely degraded by neutrophils during a period of 12 h; on the other hand, only 30% of the non-IgG-treated nanotubes were degraded (Figure 3C, D). It was found that both active hMPO and NADPH oxidase were essential for CNT degradation by neutrophils. Moreover, the *in vitro* degradation of CNTs was found to be more profound in neutrophils than in macrophages, which contain much lower level of hMPO *versus* neutrophils. Recently, Vlasova *et al.* demonstrated that PEGylated SWCNTs activated isolated human neutrophils to produce HClO, and both oxidized and PEGylated SWCNTs were determined to activate neutrophils in whole blood samples [64]. Therefore, the mechanism of CNT degradation by neutrophils stems from hMPO associated oxidative stress triggered by activated cells.

**3.2.2. The *in vitro* Degradation of CNTs by Eosinophils**—When in an inflammatory state, eosinophils are an additional type of professional phagocytes that generate oxidative species *via* EPO. In order to simulate the inflammatory conditions that are induced by CNT exposure, CNT degradation experiments were carried out in a cellular culture system with highly purified murine eosinophils that were obtained from mouse bone marrow progenitors [29]. Different from MPO, which is expressed inside neutrophils for killing bacterial cells, EPO is exocytosed from activated eosinophils and is mainly responsible for destroying parasites [44]. Degranulation and exocytosis of murine EPO (mEPO) were triggered by cytochalasin B and a platelet-activating factor (PAF). Upon 48 h incubation of carboxylated SWCNTs with activated mEPO, TEM images revealed that the bulk of SWCNT bundles were degraded leaving residual CNTs and carbonaceous materials (Figure 4A, B). The degradation was also confirmed by a decrease in both the S<sub>2</sub> band for the NIR spectra and the G-band for the Raman spectra of SWCNTs (Figure 4C–E). It was noted that the degradation of CNTs by eosinophils occurs extracellularly in contrast of degradation by neutrophils, as the mEPO is exocytosed upon cellular activation and functions by forming reactive intermediates and HBrO as described in Section 2.2.

#### 4. Biodistribution, Clearance, and Fate of CNTs *in vivo*

The biodistribution, clearance, and fate of CNTs *in vivo* are influenced by administration method, length, and functionalization of this nanomaterial. The term “clearance” mostly refers to the excretion of CNTs through lymphatic, biliary, or renal pathways [65, 66]; an alternative mechanism of CNT clearance *via* enzyme-catalyzed biodegradation *in vivo* is rarely discussed in the literature and will be the focus of Section 5. Importantly, the method by which CNTs are administered influences their biodistribution and clearance [67]. CNTs that are injected intravenously demonstrate low toxicity as a result of an opsonization regulated reticuloendothelial system (RES) capture, which minimizes the interaction of SWCNTs with parenchyma cells and restricts the toxicity to primarily the Kupffer cells (KC) and alveolar macrophages (AM) [68]. Therefore, CNT clearance mechanisms from AM and KC include either departing the lung *via* mucus through mucociliary transport [69] or being slowly excreted from KCs *via* bile [65]. On the other hand, intratracheally instilled SWCNTs and SWCNTs that were injected into the peritoneal cavity of mice induce more serious injury including inflammation and the formation of granuloma [70–72].

Depending on their length, CNTs may exhibit different pathogenic behaviors. Long fibers and large aggregates of CNTs, which are difficult for macrophages to phagocytose, typically induce asbestos-like pathogenicity including chronic inflammation and formation of granulomas and fibrosis in the lungs [72, 73]. After administration, these bulky materials often have a much longer retention time within the tissues and are not cleared. In contrast, short, functionalized CNTs tend to be more easily phagocytosed by the mononuclear phagocyte system or cleared through different pathways [66, 74, 75]. This was exemplified by the work of Kolosnjaj-Tabi *et al.* [76]. After administering SWCNTs of different lengths into Swiss mice *via* intraperitoneal injection, their data revealed that: large aggregates of SWCNTs (>10 μm) irremediably induce granuloma formation; smaller aggregates (<10 μm) were engulfed by phagocytes but remain persistent in cells for several months; and small, well-functionalized SWCNTs (<300 nm) were eliminated *via* the kidneys and bile ducts.

The surface modification of a CNT has been reported to directly affect its inflammatory response and facilitate its clearance. To this end, numerous strategies are available to reduce the size of CNTs and tune their surface properties. For example, functionalization with DNA, protein, or polymers may improve the dispersion and biocompatibility of CNTs [77–79]. Dai's group demonstrated that short SWCNTs ( $\sim 100 \pm 50$  nm) functionalized with branched PEGylated phospholipids chains exhibited a significant increase in circulation time ( $\approx 15$  h) *versus* non-branched PEGylated SWCNTs; they hypothesized that branched PEG structures on SWCNTs provided optimal biological inertness and resistance to opsonization/nonspecific binding of proteins [65]. In turn, this limited the rapid RES uptake of the SWCNTs and thus prolonged their circulation time in the blood. After 1 day of circulation, SWCNTs were predominantly located in the RES organs of the liver and spleen with uptake inversely depended on the degree of SWCNT surface PEGylation. Meanwhile, over a three month period, the concentration of SWCNTs remained very low in most of the organs except for the liver and spleen in which the concentration of SWCNTs steadily decreased over the 3-month period with retention in the spleen and liver inversely proportional to the degree of PEGylation. Because excretion of SWCNTs *via* the renal pathway was restricted to nanotubes that were very short in length (*i.e.*  $< 50$  nm in length, diameter 1–2 nm, less than the renal excretion threshold), Dai and coworkers determined that the primary mechanism for the removal of SWCNTs involved the biliary pathway as evidenced by SWCNTs being found in both the intestine and feces.

In contrast to Dai's work [65], Singh *et al.* observed rapid, first-order clearance of functionalized/water dispersible  $^{111}\text{In}$ -labeled DTPA-SWCNTs that were between 300 and 1,000 nm in length from the blood through the renal excretion pathway without any toxic side effects or mortality [80]. The difference between the observations of Dai and Singh may have stemmed from the fact that PEGylated nanotubes possess unique properties that effect pharmacokinetics, biodistribution, and clearance/fate. Recently, Sacchetti *et al.* completed a study, where they examined the effects of surface charge and PEG conformation on the adsorption of plasma proteins to SWCNTs and the resulting biodistribution [81]. Since the conformation of the PEG group affects the adsorption of the corona's major components, it was determined that the conformation of PEG had greater influence over the composition of the protein corona *versus* the surface charge imparted on a nanotube. This is important because the adsorption of certain proteins may directly influence the biodistribution of PEGylated SWCNTs.

## 5. *In vivo* Biodegradation of CNTs

### 5.1. Setting the State for Biodegradation: Inflammatory Response and Recruitment of Professional Phagocytes

Depending on their dimension, functionalization and administration methods, CNTs may introduce different levels of acute or chronic inflammation [61, 73, 82], causing fibrosis, oxidative stress, and mutagenesis [83]. CNT-induced inflammatory response is usually associated with increasing levels of cytokines and professional phagocytes such as macrophages and neutrophils [61]. For example, Muller *et al.* demonstrated that, compared with un-ground MWCNTs, MWCNTs ground with an oscillatory ball mill induced more

significant cytotoxicity and inflammatory response in lungs, accompanied with increased levels of neutrophils and eosinophils [84]. Therefore, the accumulation of professional phagocytes during inflammation is postulated to be responsible for this clearance by engulfment of CNTs [73] and/or creating oxidative environment that facilitates the biodegradation of CNTs *in vivo* [27]. This behavior was corroborated by Vlasova *et al.*, who observed both an increase in the percentage of circulating neutrophils and activation of neutrophils and macrophages in the peritoneal cavity thereby suggesting an inflammatory response after an intraperitoneal injection of PEGylated SWCNTs into mice [64]. In turn, the activated neutrophils are capable of producing high, local concentrations of HOCl, which represent favorable conditions for biodegrading the nanotubes.

## 5.2. The *in vivo* Biodegradation of CNTs in the Lung

The *in vivo* degradation of CNTs was possibly observed in a study by Elgrabli *et al.* [85]. Oxidized MWCNTs were intratracheally instilled into rat lungs at different doses. The injected MWCNTs were found to be predominantly distributed in the lungs and gradually diminished from the lung during 180 days. A significant increase in the number of alveolar macrophages (AMs), which are responsible for engulfing MWCNTs, was observed. The phagocytosis of MWCNTs by AMs was directly dependent on dosage and inversely related to time. To this end, the number of AMs that contained MWCNTs increased with an increasing dosage of MWCNTs, and as time progressed, this value gradually decreased. It was postulated that the AM cells underwent apoptosis after phagocytosis of MWCNTs and were subsequently engulfed by other AMs. The interesting finding of this study was that MWCNTs underwent both physical and chemical modification 15 days after instillation. Significant diminution of MWCNT length was noticed suggesting the cleavage of MWCNTs by rat lungs, along with the introduction of different functional groups on MWCNTs (Figure 5). Although detailed characterization and mechanism of this structural change remained vague, the authors proposed that the AMs might modify the MWCNTs upon phagocytosis and facilitate their further elimination from the lung.

In a recent collaborative study, we investigated the *in vivo* degradation of oxidized SWCNTs instilled into the lung *via* pharyngeal aspiration of either wild-type (w/t) or myeloperoxidase knockout (MPO k/o) mice (*i.e.* mice with MPO deficiency) [28]. For both types of mice, a pulmonary inflammatory response and the accumulation of neutrophils was observed as early as 1 day after exposure. While the phagocytized SWCNTs remained persistent in the neutrophils of MPO k/o mice and induced a stronger fibrogenic response, SWCNTs underwent significant diminution in the lungs of w/t mice *versus* MPO k/o mice as evidenced through quantitative imaging (Figure 6). Twenty-eight days after exposure, TEM and Raman analysis also confirmed that the oxidized SWCNTs underwent biodegradation as evidenced by the shortening of the CNTs and an increase in the ratio of the D to G bands for the respective techniques; this effect, however, was more apparent in the w/t mice, which indicated the crucial role of MPO in oxidatively biodegrading SWCNTs *in vivo* [26]. Since the degradation was also observed in MPO k/o mice at a much lower rate, other hemeperoxidases (*e.g.* EPO and LPO) may also contribute to the *in vivo* biodegradation process. In agreement with our previous *in vitro* study, the *in vivo* results strengthened the importance of MPO containing neutrophils in the biodegradation of CNTs.

### 5.3. The *in vivo* biodegradation of CNTs in the Brain

Nunes *et al.* recently investigated the fate of MWCNTs in mouse neuronal tissue [86]. Amine-functionalized MWCNTs were stereotactically injected into the motor cortex of a mouse brain, where microglia functioned as the primary professional phagocytes for the brain's immune system. TEM imaging was performed on parenchyma samples near the injection site 2 days post-injection. While widespread microglia internalization of MWCNTs was considered to be the predominant mechanism of early tissue response, the micrographs revealed that this nanomaterial was also internalized into different types of brain cells including neurons (Figure 7A). Aggregates of MWCNTs were localized in the possible phagolysosomal vesicles through active endocytosis or phagocytosis, and individualized MWCNTs were mainly internalized in the cytoplasm through a direct membrane translocation pathway. Besides the intact nanotubes, many internalized MWCNTs were observed to undergo severe structural deformation yielding amorphous debris (Figure 7B), which indicated the widespread initiation of the degradation process in microglia on day 2 after injection. This structural deformation was confirmed by Raman spectra that were taken of the injected brain tissue on days 2 and 14 after injection (Figure 7C, D, E), which demonstrated an overall reduction in the intensity of the D and G peaks coupled with an increase in background noise thereby indicating diminishing CNT content. A decrease in the D to G band ratio was observed, however, which might indicate the incomplete degradation of MWCNTs in microglia as was observed in another degradation experiment conducted on MWCNTs [23]. While the authors attributed the possible *in vivo* degradation of MWCNTs to the highly efficient phagocytosis capacity of microglia cells that possess both an oxidative lysosomal environment with low pH and an abundance of hydrolytic enzymes, the actual mechanism of degradation remained hypothetical.

## 6. Comparison to Other Nanomaterials

Unlike peroxidase-catalyzed degradation of CNTs and graphene oxide [24], the biodegradation of other nanoparticles may undergo completely different pathways depending on their chemical properties. The most inert gold nanoparticles (NPs) are rarely reported to undergo biodegradation in cells [87] with their eventual *in vivo* fate likely to include retention inside organs such as the liver and spleen [88]. In contrast, iron oxide NPs can be gradually degraded in the acidic environment of endosomes or lysosomes after cellular uptake thereby releasing ferric ions [89]. Quantum dots (QDs) such as CdSe and CdTe were also reported to undergo a pH-dependent degradation [90], and the presence of intracellular hypochlorous acid and hydrogen peroxide may facilitate the degradation process [91]. The degradation of QDs is not desired because the released Cd<sup>2+</sup> ions are highly cytotoxic, which, in turn, greatly limits the biomedical applications of QDs. Different types of inorganic NPs, which include semiconductor, metal, metal oxide, and lanthanide-doped QDs are commonly encapsulated in polymers or coated with lipids or surfactants to preserve the as-synthesized properties of the nanomaterial [92]. The surface properties of these carbonaceous coatings, which are highly vulnerable to oxidative biodegradation, will impact the interactions of NPs with cells and components of biofluids thus defining their fate and effectiveness in the body. Therefore, peroxidase-catalyzed biodegradation reactions

can affect not only carbonaceous NPs but also many other types of NPs that utilize carbon-based coatings as a part of their formulation.

A large group of biocompatible polymeric NPs has been developed as novel drug delivery vehicles such as poly(lactic acid) (PLA), poly(lactic-*co*-glycolic acid) (PLGA), *etc.*, which can be degraded through either enzymatic or hydrolytic pathways [93, 94]. Along these lines, de Gracia Lux *et al.* developed polymeric capsules that contained aryl boronic ester protecting groups integrated into their polymer design [95]. Due to the cleavage of the boronic ester by biological levels of H<sub>2</sub>O<sub>2</sub> (*i.e.* 50–100 μM), which resulted in the degradation of the polymer backbone, these nanoparticle demonstrated the ability to release cargo when incubated in physiological environments such as with activated neutrophils.

## 7. Outlook

Ideally, delivery vehicles (*e.g.* CNTs or graphene derivatives) that transport theranostic payloads should be disposed of after arriving at their target destination sites. To this end, while many chemical methodologies have been developed to “oxidatively cut” and degrade CNT, the aggressive nature of these oxidants precludes their possible employment in physiologically relevant environments (*i.e.* tissues and body biofluids). Consequently, this prompted an active search for possible enzymatic mechanisms and pathways whereby mild and controlled oxidation reactions would effectively biodegrade CNTs. The discovery of peroxidase-driven biodegradation processes is an important milestone on the path to regulated and targeted spatiotemporal degradation of CNT. Through either noncovalent functionalization or covalent attachment through stimuli-cleavable groups, specialized signaling molecules of lipid and/or protein nature will facilitate the internalization of CNTs. Also, one can envision the attachment of chemical/biological species that will activate the professional phagocytes. Acute and resolution phases of the body's inflammatory response are characterized by the predominant accumulation of myeloperoxidase (MPO)-rich PMNs and macrophages, respectively. One can envision that MPO-driven oxidative reaction will represent the dominant pathways for the CNTs biodegradation during the acute phase. In contrast, macrophages, which are relatively poor in MPO, may utilize a different oxidizing system such as peroxynitrite generators to be involved in the CNT biodegradation process. In this regard, NADPH-oxidase and NO synthases (*e.g.* iNOS) may be particularly important as sources of superoxide radicals and NO<sup>•</sup>, respectively. By producing these reactive oxygen and nitrogen species (*i.e.* ROS and RNS), macrophages are involved in the production of peroxynitrite, whose high oxidizing potential is sufficient to trigger CNT oxidative degradation. Therefore, by tailoring functionalization, one can envision a possible tool for regulating the biodegradation of CNTs coated with important payloads. Alternatively, nano-containers with encapsulated freight can be utilized in ways where oxidative biodegradation of the vehicle will facilitate the release of the inner contents as they reach the desired targets. While different types of nano-containers have been designed and fabricated [96–98], approaches towards the utilization of peroxidase-catalyzed oxidative biodegradation on these types of delivery nano-devices in target organs/cells have not yet been developed and represent an exciting future area of research.

## Acknowledgments

The project described was supported by NIEHS R01ES019304, NIOSH OH008282, and NIH U19AI068021. GPK acknowledges support from the EPA STAR Graduate Fellowship FP-91713801. YZ acknowledges a graduate student fellowship through Bayer MaterialScience.

## References

- [1]. Kim SN, Rusling JF, Papadimitrakopoulos F. Carbon nanotubes for electronic and electrochemical detection of biomolecules. *Adv. Mater.* 2007; 19:3214–3228. [PubMed: 18846263]
- [2]. Odom TW, Huang J-L, Kim P, Lieber CM. Structure and electronic properties of carbon nanotubes. *J. Phys. Chem. B.* 2000; 104:2794–2809.
- [3]. Dresselhaus MS, Dresselhaus G, Jorio A. Unusual properties and structure of carbon nanotubes. *Annu. Rev. Mater. Res.* 2004; 34:247–278.
- [4]. Ruoff RS, Lorents DC. Mechanical and thermal properties of carbon nanotubes. *Carbon.* 1995; 33:925–930.
- [5]. Avouris P, Appenzeller J, Martel R, Wind SJ. Carbon nanotube electronics. *Proc. IEEE.* 2003; 91:1772–1784.
- [6]. Kauffman DR, Star A. Carbon nanotube gas and vapor sensors. *Angew. Chem., Int. Ed.* 2008; 47:6550–6570.
- [7]. Feigel IM, Vedala H, Star A. Biosensors based on one-dimensional nanostructures. *J. Mater. Chem.* 2011; 21:8940–8954.
- [8]. Coleman JN, Khan U, Blau WJ, Gun'ko YK. Small but strong: A review of the mechanical properties of carbon nanotube-polymer composites. *Carbon.* 2006; 44:1624–1652.
- [9]. Baughman RH, Zakhidov AA, de Heer WA. Carbon nanotubes--the route toward applications. *Science.* 2002; 297:787–792. [PubMed: 12161643]
- [10]. Bianco A, Kostarelos K, Prato M. Applications of carbon nanotubes in drug delivery. *Curr. Opin. Chem. Biol.* 2005; 9:674–679. [PubMed: 16233988]
- [11]. Liu Z, Tabakman S, Welsher K, Dai H. Carbon nanotubes in biology and medicine: In vitro and in vivo detection, imaging and drug delivery. *Nano Research.* 2009; 2:85–120. [PubMed: 20174481]
- [12]. Michalet X, Pinaud FF, Bentolila LA, Tsay JM, Doose S, Li JJ, Sundaresan G, Wu AM, Gambhir SS, Weiss S. Quantum dots for live cells, in vivo imaging, and diagnostics. *Science.* 2005; 307:538–544. [PubMed: 15681376]
- [13]. De M, Ghosh PS, Rotello VM. Applications of nanoparticles in biology. *Adv. Mater.* 2008; 20:4225–4241.
- [14]. Vashist SK, Zheng D, Pastorin G, Al-Rubeaan K, Luong JHT, Sheu F-S. Delivery of drugs and biomolecules using carbon nanotubes. *Carbon.* 2011; 49:4077–4097.
- [15]. Bianco A, Kostarelos K, Prato M. Making carbon nanotubes biocompatible and biodegradable. *Chem. Commun.* 2011; 47:10182–10188.
- [16]. Kamalha E, Shi X, Mwasiagi J, Zeng Y. Nanotechnology and carbon nanotubes; a review of potential in drug delivery. *Macromol. Res.* 2012; 20:891–898.
- [17]. Qureshi SR, Sahni YP, Singh SK, Bhat MA, Dar AA, Quadri SA. Nanotechnology based drug delivery system. *J. Pharm. Res. Opin.* 2011; 1:161–165.
- [18]. Rothen-Rutishauser B, Brown DM, Pfaller-Boyles M, Kinloch IA, Windle AH, Gehr P, Stone V. Relating the physicochemical characteristics and dispersion of multiwalled carbon nanotubes in different suspension media to their oxidative reactivity in vitro and inflammation in vivo. *Nanotoxicology.* 2010; 4:331–342. [PubMed: 20795914]
- [19]. Zhang W, Zhang Z, Zhang Y. The application of carbon nanotubes in target drug delivery systems for cancer therapies. *Nanoscale Res. Lett.* 2011; 6:555. [PubMed: 21995320]
- [20]. Allen BL, Kichambare PD, Gou P, Vlasova, Kapralov AA, Konduru N, Kagan VE, Star A. Biodegradation of single-walled carbon nanotubes through enzymatic catalysis. *Nano Lett.* 2008; 8:3899–3903. [PubMed: 18954125]

- [21]. Allen BL, Kotchey GP, Chen Y, Yanamala NVK, Klein-Seetharaman J, Kagan VE, Star A. Mechanistic investigations of horseradish peroxidase-catalyzed degradation of single-walled carbon nanotubes. *J. Am. Chem. Soc.* 2009; 131:17194–17205. [PubMed: 19891488]
- [22]. Russier J, Menard-Moyon C, Venturelli E, Gravel E, Marcolongo G, Meneghetti M, Doris E, Bianco A. Oxidative biodegradation of single- and multi-walled carbon nanotubes. *Nanoscale.* 2011; 3:893–896. [PubMed: 21116547]
- [23]. Zhao Y, Allen BL, Star A. Enzymatic degradation of multiwalled carbon nanotubes. *J. Phys. Chem. A.* 2011; 115:9536–9544. [PubMed: 21348486]
- [24]. Kotchey GP, Allen BL, Vedala H, Yanamala N, Kapralov AA, Tyurina YY, Klein-Seetharaman J, Kagan VE, Star A. The enzymatic oxidation of graphene oxide. *ACS Nano.* 2011; 5:2098–2108. [PubMed: 21344859]
- [25]. Kotchey GP, Hasan SA, Kapralov AA, Ha SH, Kim K, Shvedova AA, Kagan VE, Star A. A natural vanishing act: The enzyme-catalyzed degradation of carbon nanomaterials. *Acc. Chem. Res.* 2012; 45:1770–1781. [PubMed: 22824066]
- [26]. Kagan VE, Konduru NV, Feng W, Allen BL, Conroy J, Volkov Y, Vlasova II, Belikova NA, Yanamala N, Kapralov A, Tyurina YY, Shi J, Kisin ER, Murray AR, Franks J, Stolz D, Gou P, Klein-Seetharaman J, Fadeel B, Star A, Shvedova AA. Carbon nanotubes degraded by neutrophil myeloperoxidase induce less pulmonary inflammation. *Nat. Nanotechnol.* 2010; 5:354–359. [PubMed: 20364135]
- [27]. Vlasova I, Sokolov A, Chekanov A, Kostevich V, Vasilyev V. Myeloperoxidase-induced biodegradation of single-walled carbon nanotubes is mediated by hypochlorite. *Russ. J. Bioorg. Chem.* 2011; 37:453–463.
- [28]. Shvedova AA, Kapralov AA, Feng WH, Kisin ER, Murray AR, Mercer RR, St. Croix CM, Lang MA, Watkins SC, Konduru NV, Allen BL, Conroy J, Kotchey GP, Mohamed BM, Meade AD, Volkov Y, Star A, Fadeel B, Kagan VE. Impaired clearance and enhanced pulmonary inflammatory/fibrotic response to carbon nanotubes in myeloperoxidase-deficient mice. *PLoS One.* 2012; 7:e30923. [PubMed: 22479306]
- [29]. Andón FT, Kapralov AA, Yanamala N, Feng W, Baygan A, Chambers BJ, Hultenby K, Ye F, Toprak MS, Brandner BD, Fornara A, Klein-Seetharaman J, Kotchey GP, Star A, Shvedova AA, Fadeel B, Kagan VE. Biodegradation of single-walled carbon nanotubes by eosinophil peroxidase. *Small.* 2013 DOI: 10.1002/sml.201202508.
- [30]. Veitch NC. Horseradish peroxidase: A modern view of a classic enzyme. *Phytochemistry.* 2004; 65:249–259. [PubMed: 14751298]
- [31]. Azevedo, AM.; Martins, VC.; Prazeres, DMF.; Vojinovi, V.; Cabral, JMS.; Fonseca, LP. *Biotechnol. Annu. Rev. Elsevier*; 2003. Horseradish peroxidase: A valuable tool in biotechnology; p. 199-247.
- [32]. Wepasnick KA, Smith BA, Schrote KE, Wilson HK, Diegelmann SR, Fairbrother DH. Surface and structural characterization of multi-walled carbon nanotubes following different oxidative treatments. *Carbon.* 2011; 49:24–36.
- [33]. Yang J-C, Yen C-H, Wang W-J, Horng J-J, Tsai Y-P. Assessment of adequate sodium hypochlorite concentration for pre-oxidation of multi-walled carbon nanotubes. *J. Chem. Technol. Biotechnol.* 2010; 85:699–707.
- [34]. Liu X, Hurt RH, Kane AB. Biodurability of single-walled carbon nanotubes depends on surface functionalization. *Carbon.* 2010; 48:1961–1969. [PubMed: 20352066]
- [35]. Tasis D, Tagmatarchis N, Bianco A, Prato M. Chemistry of carbon nanotubes. *Chem. Rev.* 2006; 106:1105–1136. [PubMed: 16522018]
- [36]. Sun Z, Nicolosi V, Rickard D, Bergin SD, Aherne D, Coleman JN. Quantitative evaluation of surfactant-stabilized single-walled carbon nanotubes: Dispersion quality and its correlation with zeta potential. *J. Phys. Chem. C.* 2008; 112:10692–10699.
- [37]. Hu H, Yu AP, Kim E, Zhao B, Itkis ME, Bekyarova E, Haddon RC. Influence of the zeta potential on the dispersability and purification of single-walled carbon nanotubes. *J. Phys. Chem. B.* 2005; 109:11520–11524. [PubMed: 16852411]
- [38]. Farhangrazi ZS, Fossett ME, Powers LS, Ellis WR. Variable-temperature spectroelectrochemical study of horseradish peroxidase. *Biochemistry.* 1995; 34:2866–2871. [PubMed: 7893700]

- [39]. Gratzel M. Photoelectrochemical cells. *Nature*. 2001; 414:338–344. [PubMed: 11713540]
- [40]. Choi HC, Shim M, Bangsaruntip S, Dai H. Spontaneous reduction of metal ions on the sidewalls of carbon nanotubes. *J. Am. Chem. Soc.* 2002; 124:9058–9059. [PubMed: 12149003]
- [41]. Nauseef WM. How human neutrophils kill and degrade microbes: An integrated view. *Immunol. Rev.* 2007; 219:88–102. [PubMed: 17850484]
- [42]. Hansson M, Olsson I, Nauseef WM. Biosynthesis, processing, and sorting of human myeloperoxidase. *Arch. Biochem. Biophys.* 2006; 445:214–224. [PubMed: 16183032]
- [43]. Arnhold J. Properties, functions, and secretion of human myeloperoxidase. *Biochemistry*. 2004; 69:4–9. [PubMed: 14972011]
- [44]. Davies MJ, Hawkins CL, Pattison DI, Rees MD. Mammalian heme peroxidases: From molecular mechanisms to health implications. *Antioxid. Redox Signaling*. 2008; 10:1199–1234.
- [45]. Kotchey GP, Gaugler JA, Kapralov AA, Kagan VE, Star A. Effect of antioxidants on enzyme-catalysed biodegradation of carbon nanotubes. *J. Mater. Chem. B*. 2013; 1:302–309.
- [46]. Jia G, Wang H, Yan L, Wang X, Pei R, Yan T, Zhao Y, Guo X. Cytotoxicity of carbon nanomaterials: Single-wall nanotube, multi-wall nanotube, and fullerene. *Environ. Sci. Technol.* 2005; 39:1378–1383. [PubMed: 15787380]
- [47]. Manna SK, Sarkar S, Barr J, Wise K, Barrera EV, Jejelowo O, Rice-Ficht AC, Ramesh GT. Single-walled carbon nanotube induces oxidative stress and activates nuclear transcription factor- $\kappa$ b in human keratinocytes. *Nano Lett.* 2005; 5:1676–1684. [PubMed: 16159204]
- [48]. Auffan M, Rose J, Bottero J-Y, Lowry GV, Jolivet J-P, Wiesner MR. Towards a definition of inorganic nanoparticles from an environmental, health and safety perspective. *Nat. Nanotechnol.* 2009; 4:634–641. [PubMed: 19809453]
- [49]. Shvedova AA, Pietrojusti A, Fadeel B, Kagan VE. Mechanisms of carbon nanotube-induced toxicity: Focus on oxidative stress. *Toxicol. Appl. Pharmacol.* 2012; 261:121–133. [PubMed: 22513272]
- [50]. Kagan VE, Tyurina YY, Tyurin VA, Konduru NV, Potapovich AI, Osipov AN, Kisin ER, Schwegler-Berry D, Mercer R, Castranova V, Shvedova AA. Direct and indirect effects of single walled carbon nanotubes on raw 264.7 macrophages: Role of iron. *Toxicol. Lett.* 2006; 165:88–100. [PubMed: 16527436]
- [51]. Shvedova AA, Kisin ER, Murray AR, Kommineni C, Castranova V, Fadeel B, Kagan VE. Increased accumulation of neutrophils and decreased fibrosis in the lung of nadph oxidase-deficient c57bl/6 mice exposed to carbon nanotubes. *Toxicol. Appl. Pharmacol.* 2008; 231:235–240. [PubMed: 18534653]
- [52]. Chanock SJ, El Benna J, Smith RM, Babior BM. The respiratory burst oxidase. *J. Biol. Chem.* 1994; 269:24519–24522. [PubMed: 7929117]
- [53]. Hampton MB, Kettle AJ, Winterbourn CC. Inside the neutrophil phagosome: Oxidants, myeloperoxidase, and bacterial killing. *Blood*. 1998; 92:3007–3017. [PubMed: 9787133]
- [54]. Berlett BS, Stadtman ER. Protein oxidation in aging, disease, and oxidative stress. *J. Biol. Chem.* 1997; 272:20313–20316. [PubMed: 9252331]
- [55]. Halliwell B. Oxidative stress and cancer: Have we moved forward? *Biochem. J.* 2007; 401:1–11. [PubMed: 17150040]
- [56]. Segal AW. How neutrophils kill microbes. *Annu. Rev. Immunol.* 2005; 23:197. [PubMed: 15771570]
- [57]. Zipfel M, Carmine TC, Gerber C, Niethammer D, Bruchelt G. Evidence for the activation of myeloperoxidase by f-meth-leu-phe prior to its release from neutrophil granulocytes. *Biochem. Biophys. Res. Commun.* 1997; 232:209–212. [PubMed: 9125133]
- [58]. McKenzie SE, Schreiber AD. Fc gamma receptors in phagocytes. *Curr. Opin. Hematol.* 1998; 5:16. [PubMed: 9515197]
- [59]. Konduru NV, Tyurina YY, Feng W, Basova LV, Belikova NA, Bayir H, Clark K, Rubin M, Stolz D, Vallhov H. Phosphatidylserine targets single-walled carbon nanotubes to professional phagocytes in vitro and in vivo. *PLoS One*. 2009; 4:e4398. [PubMed: 19198650]
- [60]. Cherukuri P, Bachilo SM, Litovsky SH, Weisman RB. Near-infrared fluorescence microscopy of single-walled carbon nanotubes in phagocytic cells. *J. Am. Chem. Soc.* 2004; 126:15638–15639. [PubMed: 15571374]

- [61]. Shvedova AA, Kisin ER, Mercer R, Murray AR, Johnson VJ, Potapovich AI, Tyurina YY, Gorelik O, Arepalli S, Schwegler-Berry D. Unusual inflammatory and fibrogenic pulmonary responses to single-walled carbon nanotubes in mice. *Am. J. Physiol. Lung Cell. Mol. Physiol.* 2005; 289:L698–L708. [PubMed: 15951334]
- [62]. Kam NWS, Liu Z, Dai H. Carbon nanotubes as intracellular transporters for proteins and DNA: An investigation of the uptake mechanism and pathway. *Angew. Chem.* 2006; 118:591–595.
- [63]. Neves V, Heister E, Costa S, Tilmaciu C, Borowiak- Palen E, Giusca CE, Flahaut E, Soula B, Coley HM, McFadden J. Uptake and release of double- walled carbon nanotubes by mammalian cells. *Adv. Funct. Mater.* 2010; 20:3272–3279.
- [64]. Vlasova II, Vakhrusheva TV, Sokolov AV, Kostevich VA, Gusev AA, Gusev SA, Melnikova VI, Lobach AS. Pegylated single-walled carbon nanotubes activate neutrophils to increase production of hypochlorous acid, the oxidant capable of degrading nanotubes. *Toxicol. Appl. Pharmacol.* 2012; 264:131–142. [PubMed: 22884993]
- [65]. Liu Z, Davis C, Cai W, He L, Chen X, Dai H. Circulation and long-term fate of functionalized, biocompatible single-walled carbon nanotubes in mice probed by raman spectroscopy. *Proc. Natl. Acad. Sci. U. S. A.* 2008; 105:1410–1415. [PubMed: 18230737]
- [66]. Murphy FA, Poland CA, Duffin R, Al-Jamal KT, Ali-Boucetta H, Nunes A, Byrne F, Prina-Mello A, Volkov Y, Li S. Length-dependent retention of carbon nanotubes in the pleural space of mice initiates sustained inflammation and progressive fibrosis on the parietal pleura. *Am. J. Pathol.* 2011; 178:2587–2600. [PubMed: 21641383]
- [67]. Yang ST, Wang X, Jia G, Gu Y, Wang T, Nie H, Ge C, Wang H, Liu Y. Long-term accumulation and low toxicity of single-walled carbon nanotubes in intravenously exposed mice. *Toxicol. Lett.* 2008; 181:182–189. [PubMed: 18760340]
- [68]. Owens Iii DE, Peppas NA. Oponization, biodistribution, and pharmacokinetics of polymeric nanoparticles. *Int. J. Pharm.* 2006; 307:93–102. [PubMed: 16303268]
- [69]. Yang, S.-t.; Guo, W.; Lin, Y.; Deng, X.-y.; Wang, H.-f.; Sun, H.-f.; Liu, Y.-f.; Wang, X.; Wang, W.; Chen, M.; Huang, Y.-p.; Sun, Y-P. Biodistribution of pristine single-walled carbon nanotubes in vivo†. *The Journal of Physical Chemistry C.* 2007; 111:17761–17764.
- [70]. Lam C-W, James JT, McCluskey R, Hunter RL. Pulmonary toxicity of single-wall carbon nanotubes in mice 7 and 90 days after intratracheal instillation. *Toxicol. Sci.* 2004; 77:126–134. [PubMed: 14514958]
- [71]. Warheit DB, Laurence BR, Reed KL, Roach DH, Reynolds GAM, Webb TR. Comparative pulmonary toxicity assessment of single-wall carbon nanotubes in rats. *Toxicol. Sci.* 2004; 77:117–125. [PubMed: 14514968]
- [72]. Poland CA, Duffin R, Kinloch I, Maynard A, Wallace WAH, Seaton A, Stone V, Brown S, MacNee W, Donaldson K. Carbon nanotubes introduced into the abdominal cavity of mice show asbestos-like pathogenicity in a pilot study. *Nat. Nanotechnol.* 2008; 3:423–428. [PubMed: 18654567]
- [73]. Smart S, Cassady A, Lu G, Martin D. The biocompatibility of carbon nanotubes. *Carbon.* 2006; 44:1034–1047.
- [74]. Murphy FA, Poland CA, Duffin R, Donaldson K. Length-dependent pleural inflammation and parietal pleural responses after deposition of carbon nanotubes in the pulmonary airspaces of mice. *Nanotoxicology.* DOI: 10.3109/17435390.17432012.17713527.
- [75]. Ali-Boucetta H, Nunes A, Sainz R, Herrero MA, Tian B, Prato M, Bianco A, Kostarelos K. Asbestos-like pathogenicity of long carbon nanotubes alleviated by chemical functionalization. *Angew. Chem., Int. Ed.* 2013; 52:2274–2278.
- [76]. Kolosnjaj-Tabi J, Hartman KB, Boudjemaa S, Ananta JS, Morgant G, Szwarc H, Wilson LJ, Moussa F. In vivo behavior of large doses of ultrashort and full-length single-walled carbon nanotubes after oral and intraperitoneal administration to swiss mice. *ACS Nano.* 2010; 4:1481–1492. [PubMed: 20175510]
- [77]. Singh R, Pantarotto D, McCarthy D, Chaloin O, Hoebeke J, Charalambos D, Briand JP, Prato M, Bianco A, Kostarelos K. Binding and condensation of plasmid DNA onto functionalized carbon nanotubes: Toward the construction of nanotube-based gene delivery vectors. *J. Am. Chem. Soc.* 2005; 127:4388–4396. [PubMed: 15783221]

- [78]. Kam NWS, Jessop TC, Wender PA, Dai H. Nanotube molecular transporters: Internalization of carbon nanotube-protein conjugates into mammalian cells. *J. Am. Chem. Soc.* 2004; 126:6850–6851. [PubMed: 15174838]
- [79]. Schipper ML, Nakayama-Ratchford N, Davis CR, Kam NWS, Chu P, Liu Z, Sun X, Dai H, Gambhir SS. A pilot toxicology study of single-walled carbon nanotubes in a small sample of mice. *Nat. Nanotechnol.* 2008; 3:216–221. [PubMed: 18654506]
- [80]. Singh R, Pantarotto D, Lacerda L, Pastorin G, Klumpp C, Prato M, Bianco A, Kostarelos K. Tissue biodistribution and blood clearance rates of intravenously administered carbon nanotube radiotracers. *Proc. Natl. Acad. Sci. U. S. A.* 2006; 103:3357–3362. [PubMed: 16492781]
- [81]. Sacchetti C, Motamedchaboki K, Magrini A, Palmieri G, Mattei M, Bernardini S, Rosato N, Bottini N, Bottini M. Surface polyethylene glycol conformation influences the protein corona of polyethylene glycol-modified single-walled carbon nanotubes: Potential implications on biological performance. *ACS Nano.* 2013; 7:1974–1989. [PubMed: 23413928]
- [82]. Huizar I, Malur A, Midgette Y, Kukoly C, Chen P, Ke P, Podila R, Rao A, Wingard C, Dobbs L. Novel murine model of chronic granulomatous lung inflammation elicited by carbon nanotubes. *Am. J. Respir. Cell Mol. Biol.* 2011; 45:858. [PubMed: 21398620]
- [83]. Shvedova AA, Kisin E, Murray AR, Johnson VJ, Gorelik O, Arepalli S, Hubbs AF, Mercer RR, Keohavong P, Sussman N. Inhalation vs. Aspiration of single-walled carbon nanotubes in c57bl/6 mice: Inflammation, fibrosis, oxidative stress, and mutagenesis. *Am. J. Physiol. Lung Cell. Mol. Physiol.* 2008; 295:L552–L565. [PubMed: 18658273]
- [84]. Muller J, Huaux F, Moreau N, Misson P, Heilier JF, Delos M, Arras M, Fonseca A, Nagy JB, Lison D. Respiratory toxicity of multi-wall carbon nanotubes. *Toxicol. Appl. Pharmacol.* 2005; 207:221–231. [PubMed: 16129115]
- [85]. Elgrabli D, Floriani M, Abella-Gallart S, Meunier L, Gamez C, Delalain P, Rogerieux F, Boczkowski J, Lacroix G. Biodistribution and clearance of instilled carbon nanotubes in rat lung. *Part. Fibre Toxicol.* 2008; 5:20. [PubMed: 19068117]
- [86]. Nunes A, Bussy C, Gherardini L, Meneghetti M, Herrero MA, Bianco A, Prato M, Pizzorusso T, Al-Jamal KT, Kostarelos K. *In vivo* degradation of functionalized carbon nanotubes after stereotactic administration in the brain cortex. *Nanomedicine.* 2012; 7:1485–1494. [PubMed: 22712575]
- [87]. Alkilany AM, Murphy CJ. Toxicity and cellular uptake of gold nanoparticles: What we have learned so far? *J. Nanopart. Res.* 2010; 12:2313–2333. [PubMed: 21170131]
- [88]. Chen YS, Hung YC, Liao I, Huang GS. Assessment of the *in vivo* toxicity of gold nanoparticles. *Nanoscale Res. Lett.* 2009; 4:858–864. [PubMed: 20596373]
- [89]. Arbab AS, Wilson LB, Ashari P, Jordan EK, Lewis BK, Frank JA. A model of lysosomal metabolism of dextran coated superparamagnetic iron oxide (spio) nanoparticles: Implications for cellular magnetic resonance imaging. *NMR Biomed.* 2005; 18:383–389. [PubMed: 16013087]
- [90]. Mahendra S, Zhu H, Colvin VL, Alvarez PJ. Quantum dot weathering results in microbial toxicity. *Environ. Sci. Technol.* 2008; 42:9424–9430. [PubMed: 19174926]
- [91]. Mancini MC, Kairdolf BA, Smith AM, Nie S. Oxidative quenching and degradation of polymer-encapsulated quantum dots: New insights into the long-term fate and toxicity of nanocrystals *in vivo*. *J. Am. Chem. Soc.* 2008; 130:10836–10837. [PubMed: 18652463]
- [92]. Nam J, Won N, Bang J, Jin H, Park J, Jung S, Jung S, Park Y, Kim S. Surface engineering of inorganic nanoparticles for imaging and therapy. *Adv. Drug Deliver. Rev.* DOI: <http://dx.doi.org/10.1016/j.addr.2012.1008.1015>.
- [93]. Soppimath KS, Aminabhavi TM, Kulkarni AR, Rudzinski WE. Biodegradable polymeric nanoparticles as drug delivery devices. *J. Control. Release.* 2001; 70:1–20. [PubMed: 11166403]
- [94]. Li J, Rothstein SN, Little SR, Edenborn HM, Meyer TY. The effect of monomer order on the hydrolysis of biodegradable poly(lactic-co-glycolic acid) repeating sequence copolymers. *J. Am. Chem. Soc.* 2012; 134:16352–16359. [PubMed: 22950719]
- [95]. de Gracia Lux C, Joshi-Barr S, Nguyen T, Mahmoud E, Schopf E, Fomina N, Almutairi A. Biocompatible polymeric nanoparticles degrade and release cargo in response to biologically relevant levels of hydrogen peroxide. *J. Am. Chem. Soc.* 2012; 134:15758–15764. [PubMed: 22946840]

- [96]. Chun H, Hahm MG, Homma Y, Meritz R, Kuramochi K, Menon L, Ci L, Ajayan PM, Jung YJ. Engineering low-aspect ratio carbon nanostructures: Nanocups, nanorings, and nanocontainers. *ACS Nano*. 2009; 3:1274–1278. [PubMed: 19408923]
- [97]. Oyama TG, Oshima A, Washio M, Tagawa S. Fabrication of nanobeads from nanocups by controlling scission/crosslinking in organic polymer materials. *Nanotechnology*. 2012; 23:495307. [PubMed: 23165355]
- [98]. Zhao Y, Tang Y, Chen Y, Star A. Corking carbon nanotube cups with gold nanoparticles. *ACS Nano*. 2012; 6:6912–6921. [PubMed: 22797411]

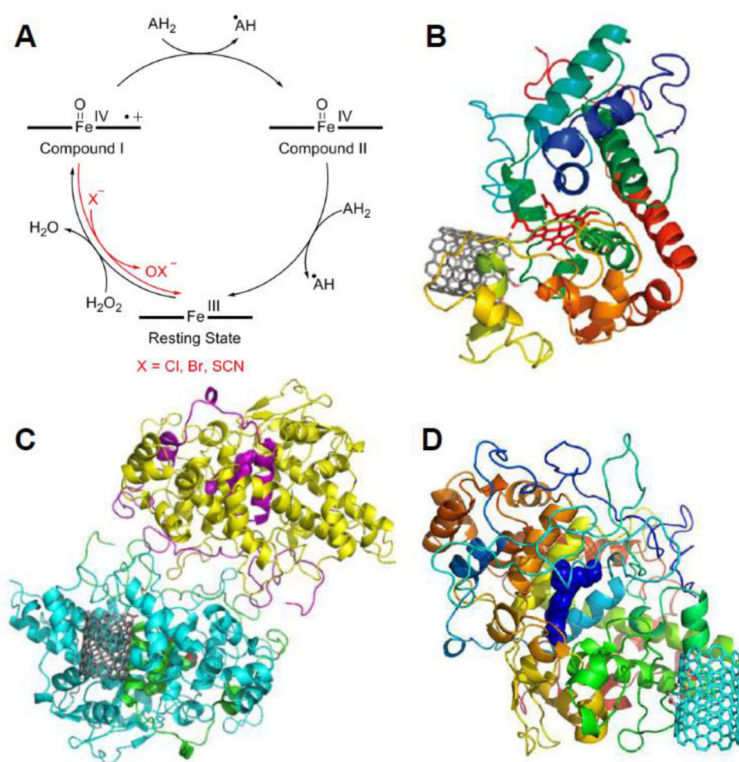


**Figure 1.**

(A) The catalytic peroxidase cycle for HRP, MPO and EPO. For MPO and EPO, compound I is reduced directly to the resting state via conversion of halide to hypohalite (red path). (B, C, D) Molecular modeling of carboxylated SWCNTs binding to the active sites of (B) HRP, (C) MPO and (D) EPO. Panel B reproduced from [21] Copyright American Chemical Society 2009, Panel C reproduced from [26] Copyright Macmillan Publishers, Ltd. 2010, and Panel D reproduced from [29] Copyright Wiley-VCH 2013.

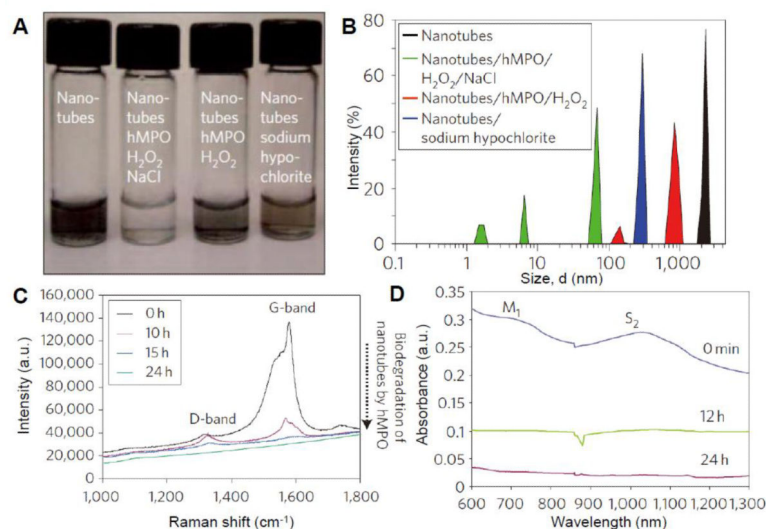


**Figure 2.**

(A) Photographs of carboxylated single-walled carbon nanotubes (SWCNTs) incubated with or without degradative reagents after 24 h. (B) Dynamic light scattering data of different samples showing decreasing sizes of degraded nanotubes. (C) Raman spectra of SWCNTs before and after 24 h of degradation by MPO/H<sub>2</sub>O<sub>2</sub>/Cl<sup>-</sup>. (D) Visible-near infrared (Vis-NIR) absorption spectra of SWCNTs being degraded during 24 h. Adapted from [26] Copyright Macmillan Publishers, Ltd. 2010.

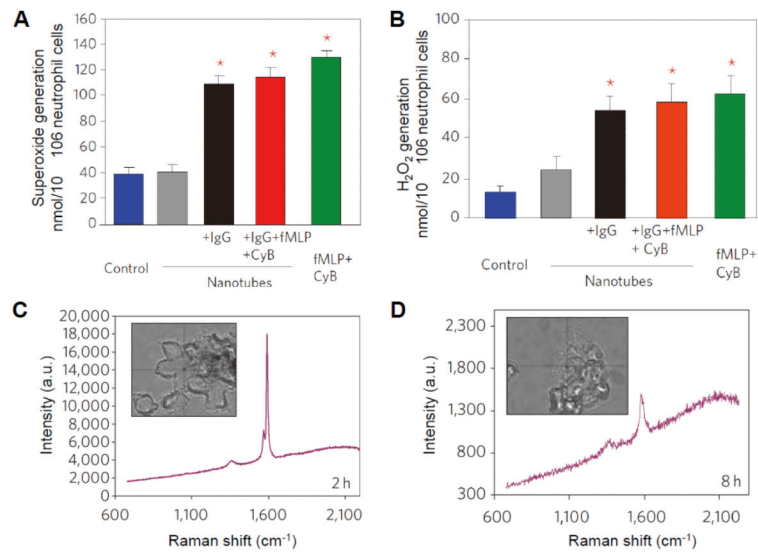


**Figure 3.**

(A, B) Quantitative assay of extracellular superoxide radicals (A) and H<sub>2</sub>O<sub>2</sub> (B) generated by activated neutrophils. \*Significant different from control (P<0.05); error bars represent standard deviations (s.d.). (C, D) Raman spectra of neutrophils containing IgG-nanotubes after 2 h (C) and 8 h (D). Adapted from [26] Copyright Macmillan Publishers, Ltd. 2010.

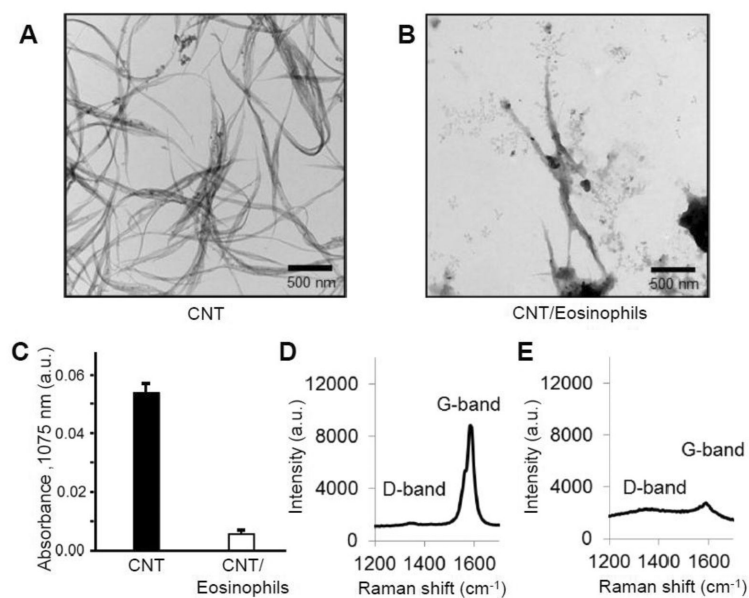


**Figure 4.** (A, B) TEM images of SWCNTs alone (A) and after 48 h of incubation with activated eosinophils (B). (C) The absorbance of S<sub>2</sub> band at 1075 nm from SWCNTs alone and SWCNTs after 48 h of incubation with activated eosinophils. (D, E) Raman spectra of SWCNTs unincubated (D) and SWCNTs incubated with eosinophils (E) showing the diminishing D and G bands. Reproduced from [29] Copyright Wiley-VCH 2013.

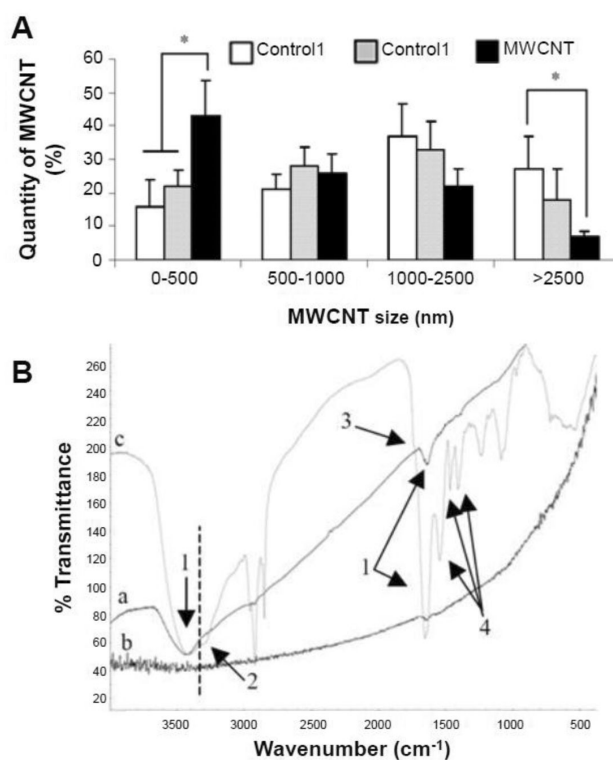


**Figure 5.**

(A) Length distribution of MWCNTs from different samples performed on at least 100 MWCNTs per sample. Control 1: MWCNTs along; Control 2: MWCNTs incubated for 15 days with suspension of lysed cells from bronchoalveolar lavage (BAL); MWCNT: MWCNTs injected to rats after 15 days. \*Significant from control ( $p < 0.05$ ); error bars represent s.d. (B) Infrared spectra of samples from (a) Control 1, (b) Control 2, and (c) MWCNTs injected to rats after 15 days. Possible peak assignment: 1. OH from H<sub>2</sub>O, 2. OH from alcohol group, 3. low quantity of carbonyl group, 4. nitrogen functional group. Reproduced from [85].

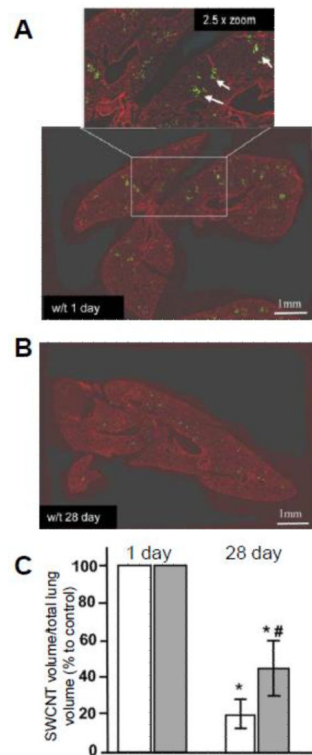


**Figure 6.**

(A, B) Quantitative imaging of the lung tissue sections from w/t mice treated with SWCNTs illustrated with green pseudo-color after 1 day (A) and 28 days (B). Inset in A - higher magnification of a field with the presence of SWCNT (green punctate spots pointed by white arrows). (C) Ratio of the volume of SWCNTs to the total lung volume for w/t and MPO k/o mice 1 day and 28 days after injection, respectively. Adapted from [28].

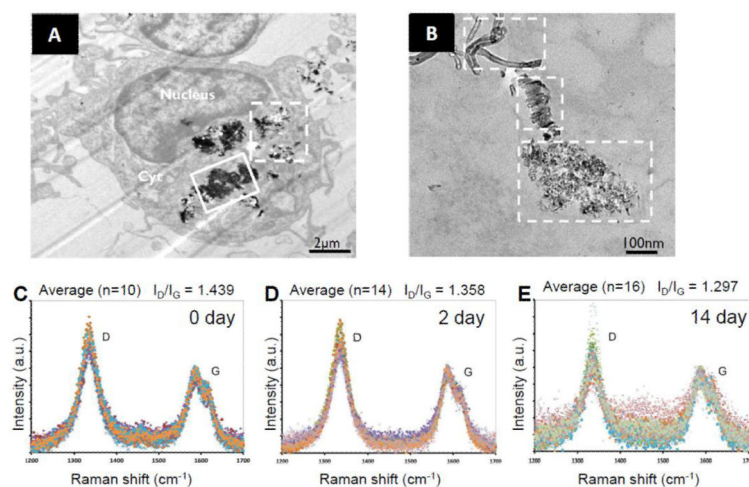


**Figure 7.**

(A) Low resolution TEM image of microglia with amine-functionalized MWCNTs localized intracellularly, both intact individualized MWCNTs (dash box) and structurally deformed MWCNT debris (solid) is exhibited. (B) TEM image with higher resolution showing co-existing intact MWCNTs (top), carbon sheets unraveled form MWCNTs (middle) and deformed MWCNT debris. (C, D, E) Raman spectra taken from the starting MWCNTs before injection and brain sections 2 days and 14 days after MWCNT injection. The corresponding D to G band ratios ( $I_D/I_G$ ) are recorded. Reproduced from [86] Copyright Future Medicine 2012.

**Table 1**

Standard Reduction Potentials (at pH 7) Along the Peroxidase Cycle for Peroxidase Involved in CNT Degradation/Biodegradation

	Standard Reduction Potentials (V)		
	HRP [39]	MPO [45]	EPO [45]
Compound I/ Resting State	--	1.16	1.10
Compound I/Compound II	0.898	1.35	--
Compound II/ Resting State	0.869	0.970	--

Author Manuscript

Author Manuscript

Author Manuscript

Author Manuscript

**Table 2**

Two-electron Reduction Potentials of (Pseudo)hypohalous Acids at pH 7 in Water [45]

Standard Reduction Potentials (V)		
HClO/Cl <sup>-</sup>	HBrO/Br <sup>-</sup>	HSCNO/SCN <sup>-</sup>
1.28	1.13	0.56

Author Manuscript

Author Manuscript

Author Manuscript

Author Manuscript